Electronic Supplementary Material (ESI) for Materials Chemistry Frontiers.

Electronic supplementary information (ESI)

Biocompatible Artificial Tendril with Spontaneous 3D Janus Multi-helix-perversion Configuration

Yingchun Su,[ab] Mehmet Berat Taskin,[b] Mingdong Dong,[b] Xiaojun Han,*[a] Flemming Besenbacher[b] and Menglin Chen*[bc]

a. State Key Laboratory of Urban Water Resource and Environment, School of Chemistry and Chemical Engineering, Harbin Institute of Technology, Harbin, 150001, China. E-mail: hanxiaojun@hit.edu.cn

b. Interdisciplinary Nanoscience Center, Aarhus University, DK-8000 Aarhus C, Denmark.

c. Department of Engineering, Aarhus University, DK-8000 Aarhus C, Denmark. E-mail: menglin@eng.au.dk

The PCL microcoils were successfully fabricated with controllable wave height and diameter through wet-electrospinning with an ethanol bath. The typical morphologies of PCL microcoils with electric field strength of 0.44 kV/cm (Fig. S1a), 0.64 kV/cm (Fig. S1b), 0.92 kV/cm (Fig. S1c) and 1.30 kV/cm (Fig. S1d) were investigated through SEM measurement, where their wave heights were marked as 420.28 μm, 215.33 μm, 120.06 μm and 70.53 μm, respectively. With varying distances between tip and collector (6, 8, 10, 12, 14, 16 and 18 cm) as well as the varying applied voltages (7, 9, 11, 13, 15 and 17 kV), the wave height and the diameter of the PCL microcoils were systematically studied, as shown in 3D plots (Fig. S1e, wave height) and (Fig. S1g, diameter). As seen in Fig. S1 e, the wave height of PCL microcoils were reduced from 507.01±108.97 to 47.10±7.28 μm as the electric field strength increased (Fig. S1f). While under different electrospinning conditions, the diameter of PCL microcoils varied from 13.94±1.96 μm to 6.36±0.44 μm. The linear relationship between the diameter of PCL microcoils and applied voltages at constant distances was shown in Fig. S1h. The diameter decreased as the voltage increased. Therefore, the wave height and diameter of coiled PCL microcoils were tunable with controlled voltages and distance.

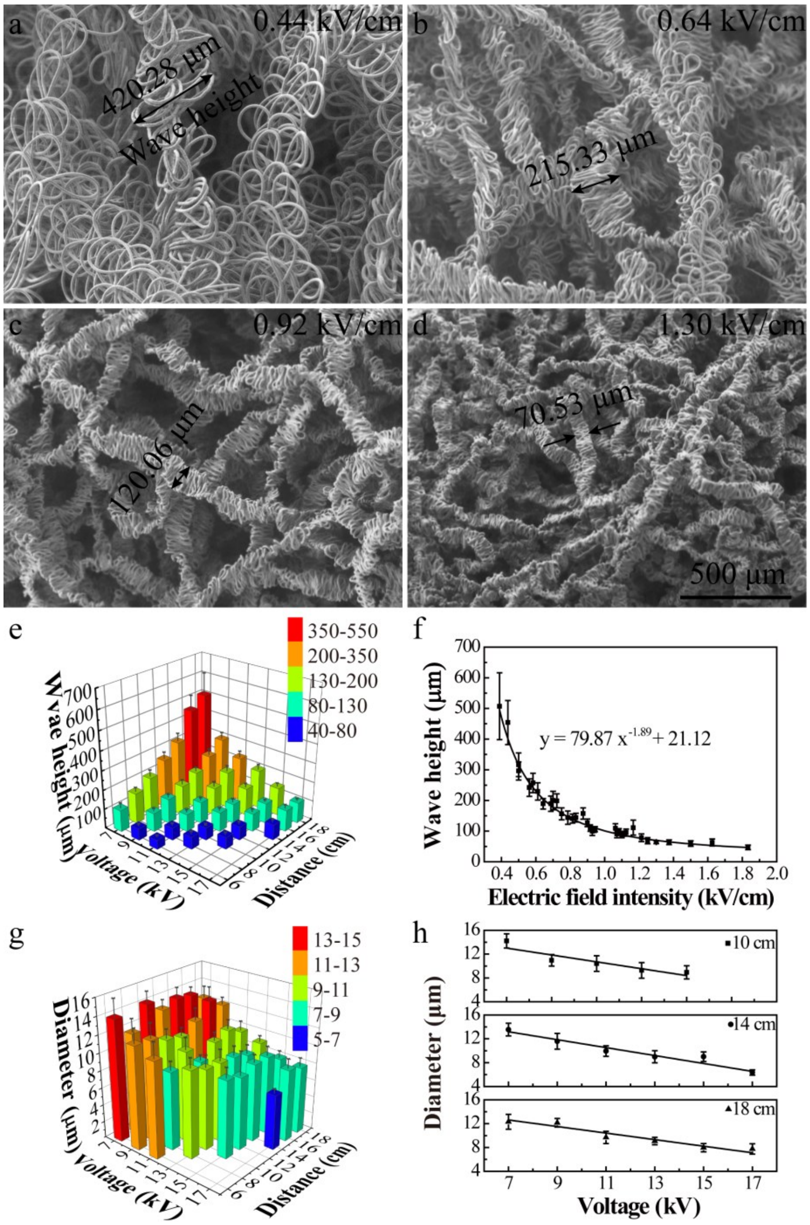

Fig. S1 The SEM images of PCL microcoils under the electric field intensity of 0.44kV/cm (a), 0.64 kV/cm (b), 0.92 kV/cm (c) and 1.30 kV/cm (d); (e) the 3D bar plot of wave height for PCL microcoils with different applied voltage and tip-collector distance; (f) the relationship between the wave height for PCL microcoils and electric field intensity; (g) the 3D bar plot of diameter for PCL microcoils with different applied voltage and tip-collector distance; (h) the linear relationship between the diameter of PCL microcoils and applied voltage with different constant tip-collector distance.

The wet electrospun PEO/PCL microstems were also observed by SEM measurement. The SEM images of PEO/PCL microstems with electrospinning condition of 9 kV and 8 cm (Fig. S2a), 11 kV and 10 cm (Fig. S2b), 13 kV and 14 cm (Fig. S2c), 15 kV and 18 cm (Fig. S2d) were presented. After collecting from the ethanol bath, the PEO/PCL microstems were compactly packed, and the surface of single PEO/PCL microstem was nanoporous, due to phase separation between PCL and PEO, as there was no preferential loss of PEO after collecting from the ethanol bath according to our previous report.[1, 2] The diameters of PEO/PCL microstems were measured from the SEM images and summarized in a 3D bar plot (Fig. S2e). The diameter of PEO/PCL microstems varied from 52.75±10.28 μm to 18.07±4.66 μm, which was significantly larger than that of PCL microcoils under the same condition, where the wave height of PCL microcoils rather than their diameter were affected mostly. The diameters of PEO/PCL microstems were affected by both applied voltage and tip-collector distance (Fig. S2f). When the applied voltage was constant, a linear diameter decrease was shown when tip-collector distance increased. While when tip-collector distance was constant, the diameter linearly decreases against the applied voltages.

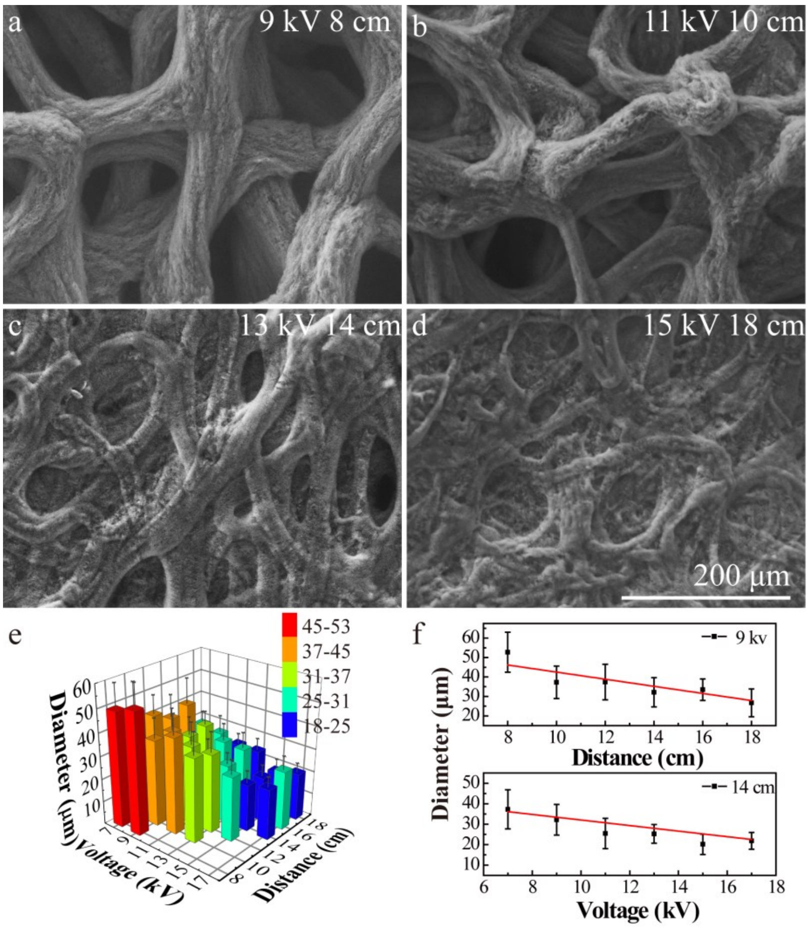

Fig. S2 The SEM images of PEO/PCL mirostems with electrospinning condition of 9 kV and 8 cm (a), 11 kV and 10 cm (b), 13 kV and 14 cm (c), 15 kV and 18 cm (d); (e) the 3D bar plot of diameter for PEO/PCL mirostems with different applied voltage and tip-collector distance; (f) the linear relationship between the diameter of PEO/PCL mirostems and tip-collector diatance at 9 kV of applied voltage as well as the applied voltage with a constant tip-collector distance of 14 cm.

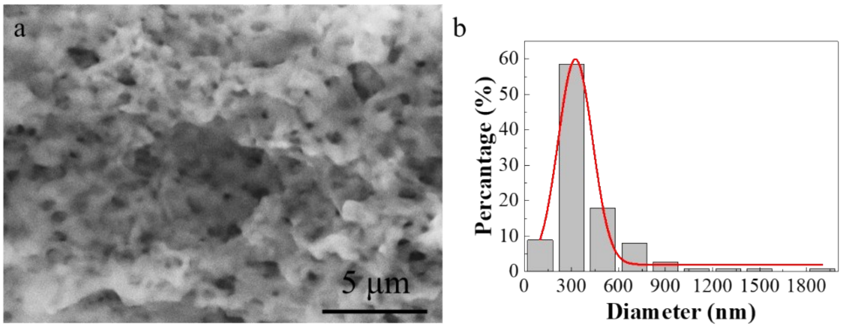

Fig. S3 (a) SEM images of PEO/PCL electrospun microstems at 9 kV 14 cm with a flow rate of 3 mL/h. (b) Diameter distribution analyzed by Gaussian fitting for the pores on PEO/PCL electrospun microstems.

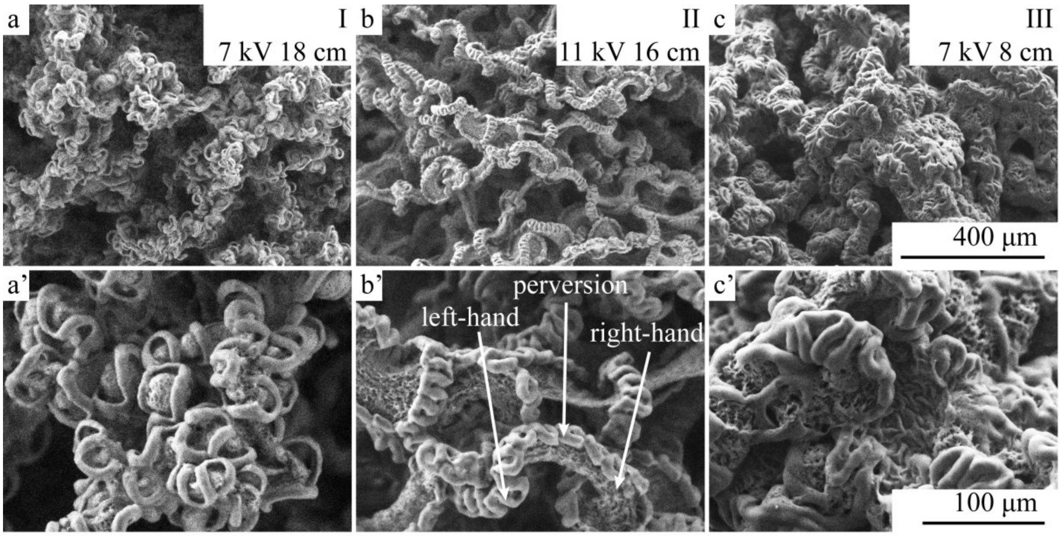

Fig. S4 SEM images of side-by-side electrospun fibers with different morphologies at 7 kV 18 cm (a), 11 kV 16 cm (b) and 7 kV 8 cm (c) with a fixed flow rate of 3 mL/h.

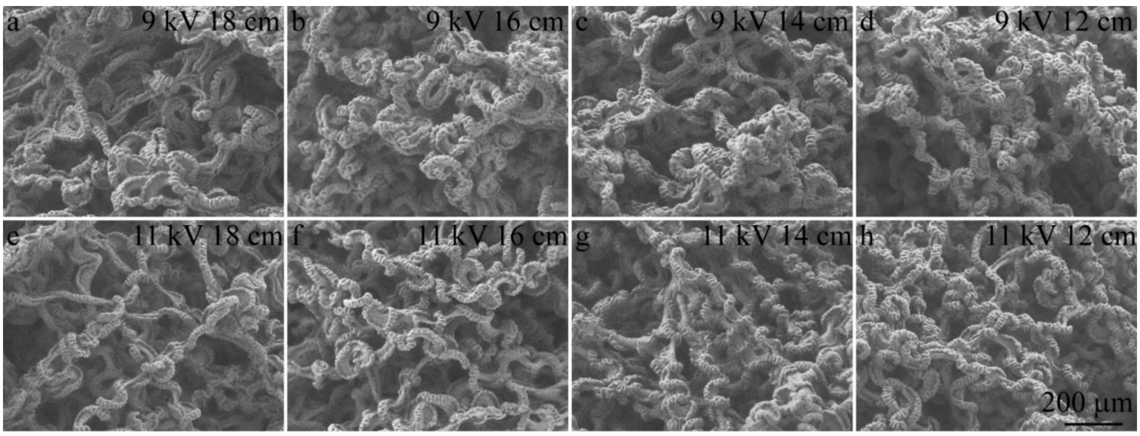

Fig. S5 SEM images of multi-helix-perversion side-by-side microfibers at different electrospining condition (region II).

Table S1 Summarized mechanical properties of single electrospun PCL microcoils, single electrospun PEO/PCL microstems, and side-by-side multi-helix-perversion microfibers.

Samples	Young's modulus (Mpa)	Ultimate tensile strength (Mpa)	Fracture point
PCL	0.34±0.10	0.13±0.04	--
PCL/PEO	13.05±6.52	1.64±0.54	49.00±19.02%
Side-by-side	3.85±1.38	0.78±0.09	~100%

For differential scanning calorimetry measurement, pure PEO powders were also tested as a comparison.The second heating process shows all the blends present the separate melting peaks of PCL around 58 °C and PEO at about 65 °C, confirming the immiscibility and phase separation, which is correlated with our previous study.[2, 3] As the PEO content decreased and the PCL content increased, the intensity of the melting peak of PEO became smaller and the peak of PEO became larger. The small shifts between the melting peaks indicated that the melting of PCL was suppressed showing a higher melting temperature, while the melting of PEO was promoted showing a lower melting temperature.

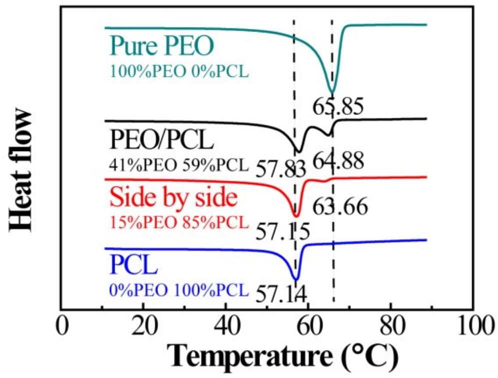

Fig. S6 The differential scanning calorimetry (DSC) measurement for pure PEO powder, single electrospun PEO/PCL microstems, side-by-side microfibers and single electrospun PCL microcoils.

Referneces

1 M. B. Taskin, D. Xia, F. Besenbacher, M. D. Dong and M. L. Chen, Nanotopography featured polycaprolactone/polyethyleneoxide microfibers modulate endothelial cell response, *Nanoscale*, 2017, **9**, 9218-9229.

2 Y. F. Li, M. Rubert, H. Aslan, Y. Yu, K. A. Howard, M. D. Dong, F. Besenbacher and M. L. Chen, Ultraporous interweaving electrospun microfibers from PCL-PEO binary blends and their inflammatory responses, *Nanoscale*, 2014, **6**, 3392-3402.

3 Y. F. Li, H. Gregersen, J. V. Nygaard, W. L. Cheng, Y. Yu, Y. D. Huang, M. D. Dong, F. Besenbacher and M. L. Chen, Ultraporous nanofeatured PCL-PEO microfibrous scaffolds enhance cell infiltration, colonization and myofibroblastic differentiation, *Nanoscale*, 2015, **7**, 14989-14995.